ISSN 2176-5480

THERMAL ANALYSIS OF CONVECTION LOSSES BY CHANGING BAFFLE SPACING IN A CAVITY

Rafael Paiva Garcia
Laura Elisa Bollini
Alcides Padilha
Vicente Luiz Scalon
Departamento de Engenharia Mecânica - UNESP/FE
Av. Luis Edmundo Carrijo Coube, 14-01, Vargem Limpa – CEP: 17033-360, Bauru(SP)
rafael.paivag@gmail.com, laura_lah@yahoo.com, padilha@feb.unesp.br, scalon@feb.unesp.br

Abstract. Energy availability and sustainability are a great preoccupation of civilization once, currently, the largest percentage from which is consumed comes from fossil fuels, such as coal, natural gas and oil. Nuclear energy, although it's a "clean" energy, it is a concern due to accidents in nuclear power plants. In this scenario, renewable energy have a very important role. Hydroelectric, biomass, wind, geothermal and solar are the solution of the energy future. However, when analyzing each one of these, one can conclude that their efficiencies change for different regions in world. When combined, as occurs in coastal areas where winds and solar radiation have good periods intercalated, one complement each other, and a symbiotic relationship could be verified. By other way, increases on thermal efficiency each one of this devices could reduces the fossil fuels dependency too. This work focuses on studying geometric changes that applied to flat plate solar collectors can improve its efficiency. The main idea is reduce the space for the convection including baffles on air-glass gap and, thus, reducing the heat losses. The influence on heat losses for different baffles spacing and possible air leaks are evaluated and discussed. Nusselt number behavior are showed by the positions on flat plate for different geometries. Results can lead to the optimal economic cost that minimizes heat losses.

Keywords: *Transparent Thermal Insulation, Flat Plate Solar Collector, Natural Convection.*

1. INTRODUCTION

Various historical events show that energy availability is proportional to the improvement in life conditions on Earth. Although, energy availability is better off than a few decades ago, environmental problems have increased demand for renewable energy, including solar power. Currently, the flat solar collectors used on solar domestic hot water systems (SDHWS) are one of the most used devices on solar energy exploitation worldwide. The efficiency of these devices is related to its ability to absorb energy without significant loses to the external environment. Thus, the thermal collector insulation is a determining factor in their efficiency. The insulations of collector lower surface and sides are easily solved using larger thicknesses of thermal insulation, the more significant problem are heat losses through the top surface. The top surface is also responsible for capturing thermal energy by radiation and, so, can not receive traditional insulations. Various schemes have been designed to reduce this heat loss and the most common one is using one or more glass cover over the absorber plate. This scheme is the most used nowadays, but several alternative techniques have been tested to improve this insulation. Most of these attempts involve using transparent insulation materials (TIM), in order to try improvements on solar collectors efficiency in general.

Studies involving insulation in transparent surfaces of systems and use of transparent insulation material has a long history. Several researches have been devoted to this subject were produced in past decades, just to mention Hollands (1965), Buchberg & Edwards (1976) and Malhotra, Garg & Rani (1980). A more detailed history of this evolution can be seen in Wong, Eames & Pereira (2007). Also around this time were produced several studies focused on determining the heat transfer coefficient in the cavity formed between collector and glass cover. Working with this theme, Hollands developed an expression that is used yet to evaluate the loss heat transfer coefficient in natural convection problems presented by Hollands et al (1976). This expression can be found in several heat transfer and solar energy textbooks as Incropera et al (2008). Subsequent to this work, other similar one was developed by Ruth, Hollands & Raithby (1980).

There are some alternatives for transparent insulation materials and all of them can minimize convection heat losses from collectors. However, everyone also reduces the collector transparency, decreasing the incident radiation on the surface of collector absorber plate. Studies have been done to determine the air thickness on cavity under the glass plate and minimize the heat loss to the environment. Steinfeld & Schubnell (1993) examined various conditions and presenting a figure for determining the heat loss based on air thickness for a given temperature.

A geometry which is commonly used in this type of devices is the honeycomb. A large number of studies have been conducted to determine its effects on the process of heat exchange using this geometry as insulator. Citing some works that treat this theme, one can highlight Sharma & Kaushika (1987), Platzer (1992), Hollands & Iynkaran (1993), Kaushika & Sharma (1994), Kaushika et al (1994), Arulanantham & Kaushika (1996) and Avanti, Arulanantham & Kaushica (1996). This geometry has been widely studied and, despite some good results, it has not been effectively

ISSN 2176-5480

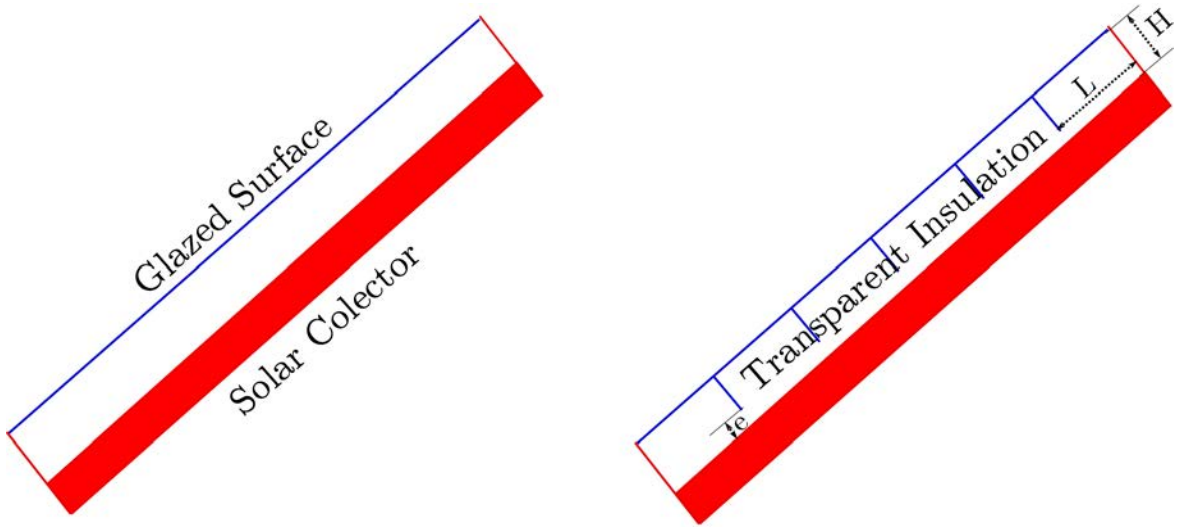

Figure 1: Changes in collector design for proposed transparent insulation.

implemented in devices. General studies for use of this type of material has been directed for air heating collectors that operate at lower temperatures but allow you to manufacture with conventional polymers. A number of problems associated with implementing this type of material have been reported by Wong, Eames & Pereira (2007) are related to degradation of the material and time required for payback. Some studies involving silica gel plates and grain as transparent insulation material can also be found in the literature as highlighted by Kaushika & Sumathy (2003).

This paper intends to present a different transparent insulation scheme to study the influence of spacing between plates on a transparent insulation system. To aim this objective it is intended to elaborate a numerical simulation for different geometric situations and baffle spacing. The models will have their limits established and, further, mesh will be generated. The boundary conditions established will be similar in all cases. In the case of solar flat plate collectors, some difficulty on creating the barriers are expected, once it's necessary a complex cut which surrounded the tubes. Because of this, the physical model presented predicts the existence of a free circulation region on the inferior part of the cavity. Figure (1) presents an scheme of the solar collector cavity with and without the transparent insulation. The numerical models are simulated using a finite volume method through the software *OpenFoam®*. Results for different baffle spacing could help to determine the best conditions of thermal insulation.

2. NUMERICAL SIMULATION

The numerical simulation needs several steps to its finalization, and that in each case is necessary mesh conception, boundary conditions establishment, mesh generation and transient simulation. Beyond this taskes, other simulation details must be defined, such as the turbulent treatment, the solution scheme, the matricidal system. Inicially, the general characteristics of the model will be approached and then the procedures that need to be altered with the geometrical changes should be detailed.

Case structure

Each case studied on OpenFoam depends on a correct directory structure. Each one of the directory must contain patronized elements, such as names and specific informations which define since the basic structure until the procedures used on the simulation. On this structure are also stored the results on times determined by the configurations archive. It is common to use ready directory structures from a previous case and alter the conditions to the case to be studied.

Depending on the solution parameters of the problem, a certain number of archives are necessary. Not only the archives, but the case and characteristics needed to the solution implicate on an use of a different computational code. To the studied case, where are evolved the coupling between the fluid flow and the heat transfer, the codes *buoyantBoussinesqPimpleFoam*, *buoyantBoussinesqSimpleFoam*, *buoyantPimpleFoam*, *buoyantSimpleFoambuoyantSimpleRadiationFoam* can be used.

In this case were used the Boussinesq types of forces and considering that the transient results could be interesting in the future, it was decided for the *buoyantBoussinesqPimpleFoam* solution.

On the directory structure it must iniciate with a main directory which contains the case's name that will be the base to the program execution. This main directory must yet contain the following subdirectories:

- ✔ *constant*: where the informations about fluid's physical properties are provided, the turbulent model, the module and direction of the gravity acceleration and a subdirectory called polymesh, where are included all the

ISSN 2176-5480

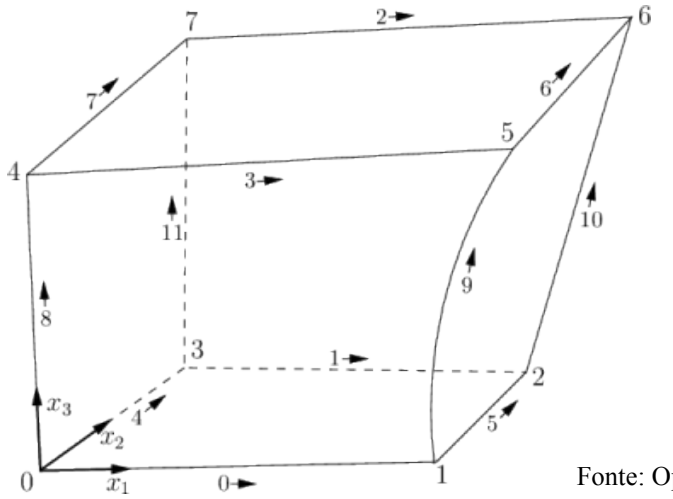

Fonte: OpenFoam, (2012)

Figure 2: Block structure for use with *blockmesh*.

informations about the mesh and the boundary surfaces.

- ✔ *system*: where are included the files that contain informations about the solution processes, such as the specific techniques to an interactive solution of the matricidal variables, inicial time, time pass and final. In this subdirectory are found three files:
  - *fvSchemes*, where are provided the informations about the interpolation scheme of each variable;
  - *fvSolution*, where are informed the solution techniques that will be applied on each equation;
  - *controlDict*, where are informed the global parameters of the solution like initial and final times;
  - *decomposeParDict*, file used only if the solution is parallelized expliciting the number of subdivisions.
- ✔ times: are various directories which represent the solution on a determined time. The directory name is the numerical value of the considered time.

Mesh grid

Mesh grid

To concept the mesh was used OpenFoam's own mesh generator named *blockmesh*. The *blockmesh* can operate with one or more blocks and all of them must obey the numerical order established on the user's manual. Figure (2) provides a typical numeration system as shown on OpenFoam, (2012). For the mesh to be defined correctly, the nods numeration system must be associated to its respective tridimensional coordinates. All this informations about the mesh are included on a file named *blockmesh.dict*, located inside the *polymesh*. Although the problem is being treated bidimensionally, tridimensional blocks were created to allow the simulation.

If only one block presents certain care, the concern must be even bigger if the final mesh involves several blocks. To simplify the generation problem, a scheme which each cavity is represented by two stacked blocks, as a way of representing the regions that contain the separators. Modifying the region's size and coupling the regions to its neighborhood, the cavities can be formed. As the *blockmesh.dict* doesn't allow the variable use, an script named m4 was used to generate the mesh.

In this case, the solid surface which separates the cavities needs to be included and it requires an addicional procedure. In this case, it was chosen the use of a “fake point” over the block to allow the appearance of the separation surface between cavities. A scheme showing this can be seen on figure (3). On this same figure it is possible to notice that the size of the mesh was arranged in such way that can't verify large discrepancies between the two blocks.

A similar procedure was done to every cavity. In these cases, the lengh and height of the geometry were kept. In this way, the increase of the cavity number implies on a smaller distance between walls. The spacing to the free flow on the below of the geometry was kept too.

ISSN 2176-5480

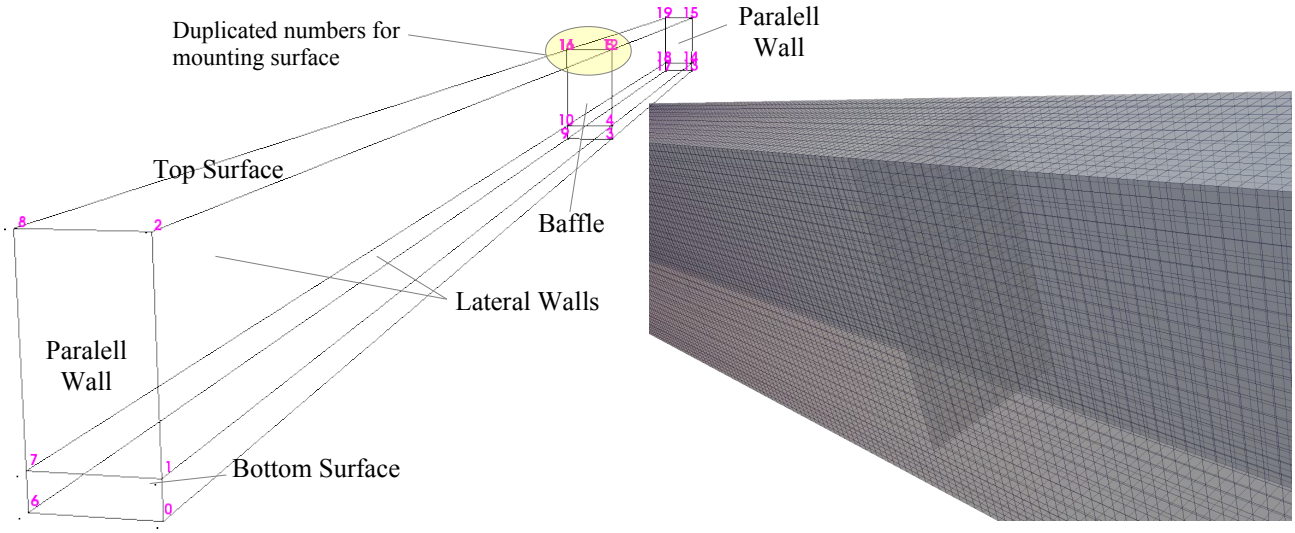

Figure 3: Blocks for mesh mounting and detail of the baffle region.

Physical model

In possession of the mesh, it is needed to adjust the physical model to the expected conditions. The following hypothesis were considered:

- ✔ Transient flow, to obtain the stationary condition.
- ✔ Boussinesq approach, although the specific mass is treated constant, its thermical expansion coefficient is used to determine the thrust forces over the fluid.
- ✔ Physical properties of the air were admitted constant $\nu=10^{-5}$ m²/s, $\beta=3.3 \times 10^{-3}$ 1/K e Pr=0.7 ;

As for the flow regime on the natural convection it was adopted laminar. As verification for this hypothesis was used a turbulent case but the turbulent energy wasn't significant. All cases were treated as laminar flow.

The solver that fits the best to the physical conditions is *buoyantBoussinesqPimpleFoam*, that will be used in the problem's solution. This solver uses a method called PIMPLE that is a coupling between tradicional method PISO and SIMPLE. OpenFoam uses the finite volume method with a technique for separation of equations to correct the pressure. Based on this procedure, theNavier Stokes equations associated to energy balance sere used for dolution and are presented on equations (1) a (5),

$$\frac{\partial u}{\partial x}+\frac{\partial v}{\partial y}+\frac{\partial w}{\partial z}=0 \tag{1}$$

$$\rho\cdot\left(\frac{\partial u}{\partial t}+u\cdot\frac{\partial u}{\partial x}+v\cdot\frac{\partial u}{\partial y}+w\cdot\frac{\partial u}{\partial z}\right)=\mu\left(\frac{\partial^2 u}{\partial x^2}+\frac{\partial^2 u}{\partial y^2}+\frac{\partial^2 u}{\partial z^2}\right)-\frac{\partial P}{\partial x}-[(\rho-\rho_\infty)\cdot g]_x \tag{2}$$

$$\rho\cdot\left(\frac{\partial v}{\partial t}+u\cdot\frac{\partial v}{\partial x}+v\cdot\frac{\partial v}{\partial y}+w\cdot\frac{\partial v}{\partial z}\right)=\mu\left(\frac{\partial^2 v}{\partial x^2}+\frac{\partial^2 v}{\partial y^2}+\frac{\partial^2 v}{\partial z^2}\right)-\frac{\partial P}{\partial y}-[(\rho-\rho_\infty)\cdot g]_y \tag{3}$$

$$\rho\cdot\left(\frac{\partial w}{\partial t}+u\cdot\frac{\partial w}{\partial x}+v\cdot\frac{\partial w}{\partial y}+w\cdot\frac{\partial w}{\partial z}\right)=\mu\left(\frac{\partial^2 w}{\partial x^2}+\frac{\partial^2 w}{\partial y^2}+\frac{\partial^2 w}{\partial z^2}\right)-\frac{\partial P}{\partial z}-[(\rho-\rho_\infty)\cdot g]_z \tag{4}$$

$$\frac{1}{\alpha}\cdot\left(\frac{\partial T}{\partial t}+u\cdot\frac{\partial T}{\partial x}+v\cdot\frac{\partial T}{\partial y}+w\cdot\frac{\partial T}{\partial z}\right)=\left(\frac{\partial^2 T}{\partial x^2}+\frac{\partial^2 T}{\partial y^2}+\frac{\partial^2 T}{\partial z^2}\right) \tag{5}$$

The approaching methods of each term of the equations can be established independently such as the solution scheme. In this case, all magnitudes evaluated were discretized with an upwind scheme using central differences when it is about diffusive or laplacian terms.

As for the matricidal solution schemes was used the Conjugated Gradients scheme with a tolerancy of 10^{-8} for pressure. The same method was used, but it was adapted to 10^{-6}. The mesh used was orthogonal and it wasn't used any corrections to compensate this kind of deviations.

ISSN 2176-5480

Table 1: Boundary conditions and defintions on surfaces

Surfaces	Type	Velocity	Temperature	Pressure (p_rgh)
Baffles and parallel walls	wall	Type fixedValue; value uniform (0 0 0);	type zeroGradient;	Type BuoyantPressure; gradient uniform 0; rho rhok; value uniform 0
Top surface	wall		type fixedValue; value uniform 300	
Bottom surface	wall		type fixedValue; value uniform 373	
Lateral walls	empty	empty		

Boundary Conditions

The boundary conditions were established on a grouped way. Figure (3) presents, beside the block assembly scheme, the position of each surface according to the description. So, according to the nature of the problem, the walls were modeled with this conditions showed on equation (6).

$$
\begin{aligned}
&-\text{Velocities:}\begin{cases}\text{Lateral walls}: \dfrac{\partial u}{\partial z}=\dfrac{\partial v}{\partial z}=0, w=0 \ \text{(simmetry)}\\ \text{All others}: u=v=w=0 \ \text{(non-slip)}\end{cases}\\
&-\text{Temperature:}\begin{cases}\text{Baffle, lateral and paralell walls}: \dfrac{\partial T}{\partial \vec{n}}=0 \ \text{(adiabatic)}\\ \text{Top surface}: T=300\,\text{K (specified temperature)}\\ \text{Bottom surface}: T=373\,\text{K (specified temperature)}\end{cases}\\
&-\text{Pressure: static distribution}
\end{aligned}
\tag{6}
$$

Using OpenFoam, when defining the surfaces (*patches*) and its names, can make a surfaces couping that have the same conditions. The surface group was formed using the nods numbers that got together to compose the surface. The couping was made, representing the boundary conditions on equation (6) and expressed in a way presented on table (1).

With the boudary conditions defined, it is needed to define the initial condition on the directory **0**. To this case were initialized the variables *T*, *U*, *p*, *p_rgh* e *kappat*, which represent temperature, pressure, preessure– *ρgh* and turbulent diffusivity. To this code, the turbulent diffusivity must be defined even when it doesn't use the turbulent mode. In this case, the turbulent diffusivity didn't change through the simulation.

3. RESULTS AND DISCUSSIONS

The results for models without divisions and for one to four divisions was obtained for verifying the influence of this baffles on global coefficient of losses of surface. It was used temperatures of 300K for top and 373K for the bottom surface. The inclination of geometry was adopted as 30° with horizontal. The inclination angle was implemented by decomposing gravitational acceleration in its components over a horizontal mesh. Variations of baffle/bottom surface spacing, Rayleigh number (caused by changes in temperatures difference) and geometry inclination were not investigated yet. Only changes in numbers of baffles was tested. For analyzing this influence on fluid dynamic, temperature profiles and Nusselt number changes some results was plotted and discussed.

Figure (4) shows the behavior of vertical velocity v on a horizontal line at the center of studied geometry. Observing this result, it is possible visualize a tendency of velocity enhancement on the wall surrounds with increasing in number of cavities. The wall induces recirculation, causing an upward movement in regions where they are found. The most significant changes in velocities occur on positions where are the baffles. The figure shows also that significant changes in the profile are verified with inclusion of the third cavity.

Then, a similar analysis considering a vertical line on center of intermediate cavity (or one of them when an even number subdivisions are considered) can be seen in figure (5). Consistent with previous results, this case also has substantial changes with third cavity inclusion. Changes lead to velocity intensification near walls. The composition of these results indicated that, in these cases, a reverse circulation region in the central region. This flow intensification near wall tends to enhanced the heat exchange process, which would not be beneficial in these cases.

ISSN 2176-5480

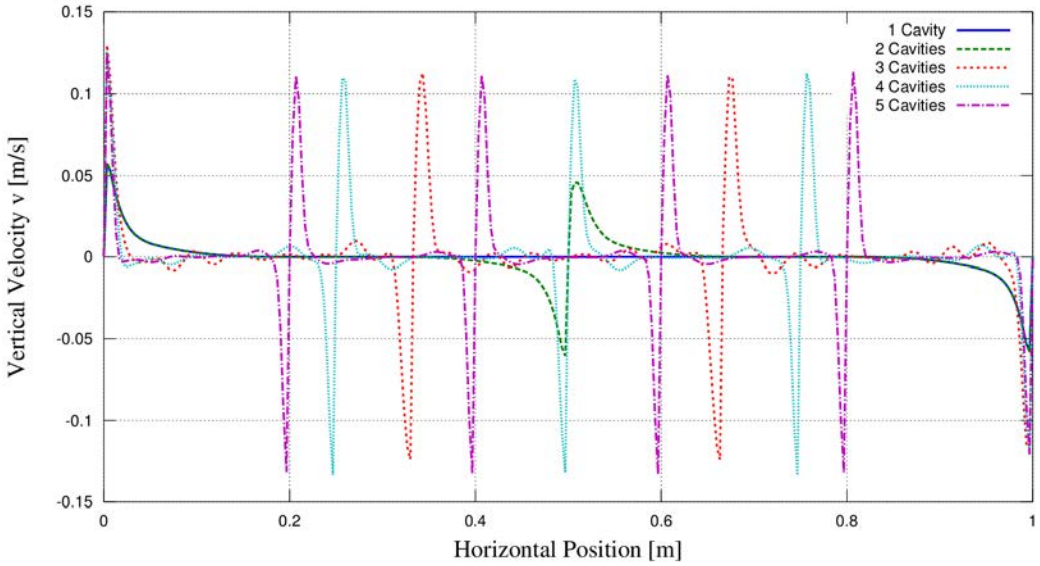

Figure 4: Vertical velocity profile on geometry centerline (y=0.02m).

An overview of changes in velocities and temperatures profiles for all simulated cases could be seen on figure (6). As can be seen on this figure, the separators induce more recirculation on the interior of the air layer. As the velocity scales were kept the same on all cases, and the vectors sizes are proportional to the velocity, one can use the figure to evaluate the changes in the flow.

It is notable that velocity on the horizontal direction increases from the case where three cavities are used. In this case it is also noted that there is a high concentration of velocity on the walls, making the flow less significant. In terms of temperature distribution. It is noted that, as increasing the number of cavities, increases the number of regions with high temperatures on the cover surface too.

As can also be seen in this figure, the baffles induce formation of an equal number of recirculations within the air layer. As scale used for velocity vector is kept constant for all geometries, so this figure can be used to evaluate changes in the flow pattern in different geometries. Note that the y-direction velocity (v) increases substantially from the case where three baffles are used. In this case, one find also a concentration of higher velocities near the walls, making the flow in the central region negligible. Considering temperature distribution, it is noted that larger number of cavities implies in greater number of regions with high temperatures on cover surface. The influence of these changes in characteristics flow and temperatures fields on heat exchange of bottom and upper surface will be analyzed later.

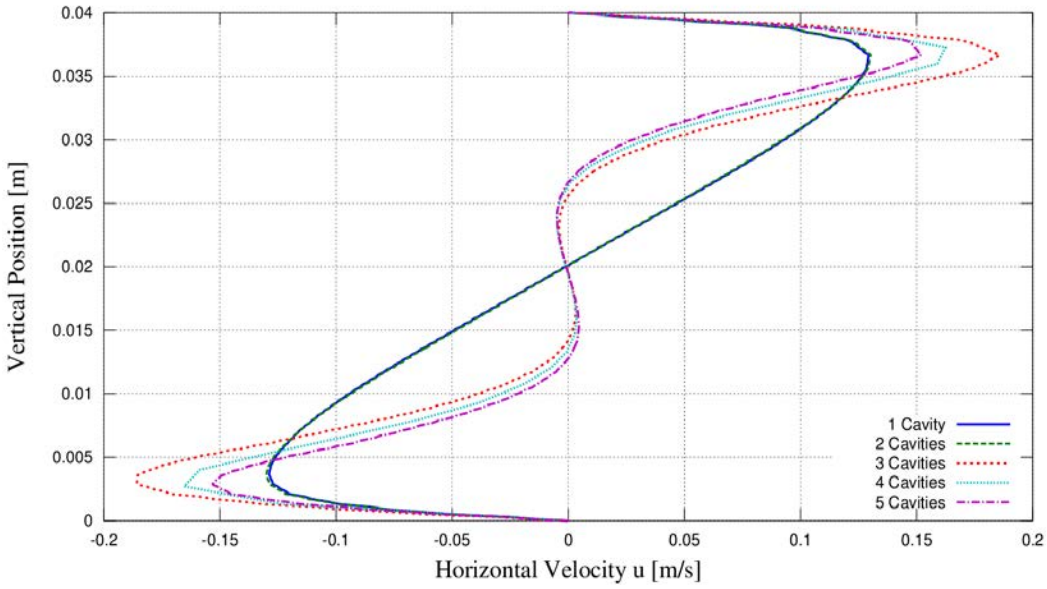

Figure 5: Horizontal velocity profile on cavity centerline considering vertical direction (*x* varying).

ISSN 2176-5480

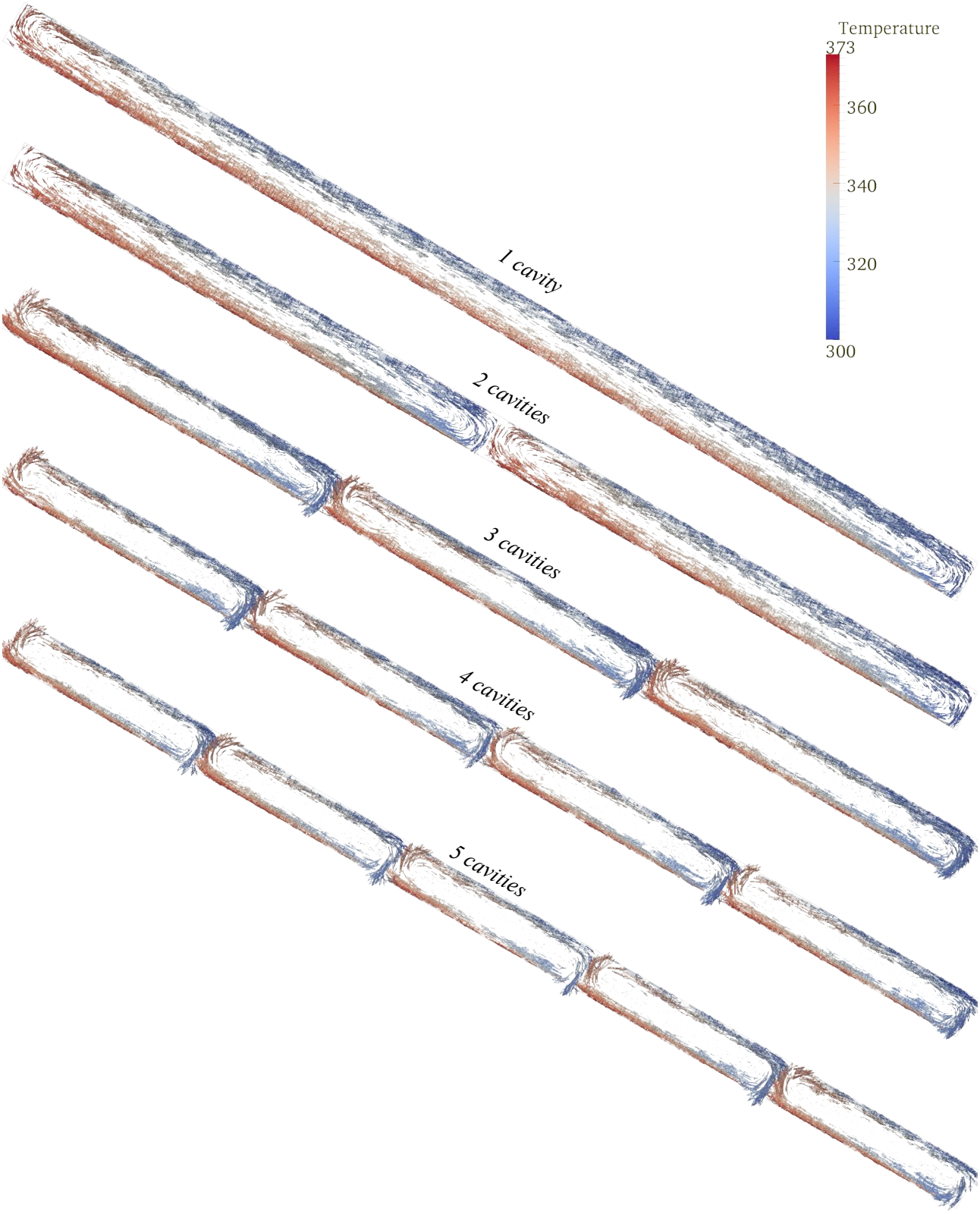

Figure 6: Velocity arrows colored by temperature for different cavities number.

ISSN 2176-5480

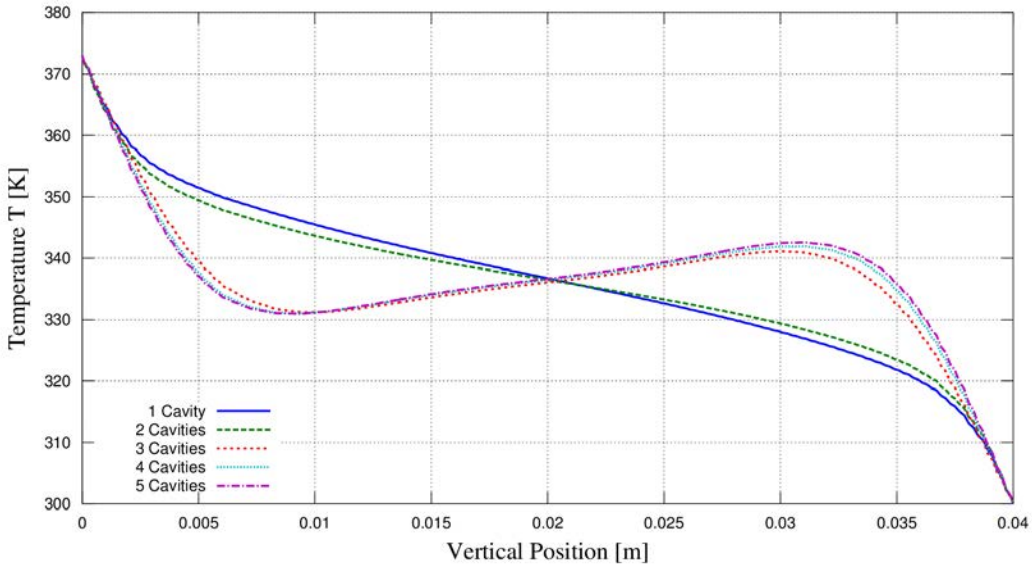

Figure 7: Horizontal temperature profile on cavity centerline considering vertical direction (x varying).

Complementing the velocity profiles for the vertical center line, shown in figure (5), the figure (7) shows the temperatures field at the same position. Observing this figure one can note the same trend reversal present on previous chart. This behavior corroborates the idea from formation of reverse recirculation at the cavity center. Despite the wide variation in the temperature profile in the central region the temperature gradient is similar to wall on all cases analyzed. Thus, no tendencies indicating major changes in the heat lost rate by the lower wall was noted.

Results for the Nusselt number behavior on the bottom surface of compound geometry can be seen on Figure (8). The baffles influence is clearly noticed. There is a significant increase in heat exchange region where the fluid is moving upward in contrast to the reduction occurred in the region where motion is downward. As seen on figure (4), , this one identifies the regions with velocities increases associated with baffles. The cavity lower region has always the lowest Nusselt numbers values. Regions near the cavities top tend to present the maximum values for Nusselt number by upward movement. There are no significant differences for various maximum values on same cavity geometry. Geometries with different numbers of cavities present greater variations of maximum values for Nusselt number. In the central region from each cavity, which forms the reverse recirculation, there is a decrease in the Nusselt number and hence for heat exchange from the geometry with three cavities or more.

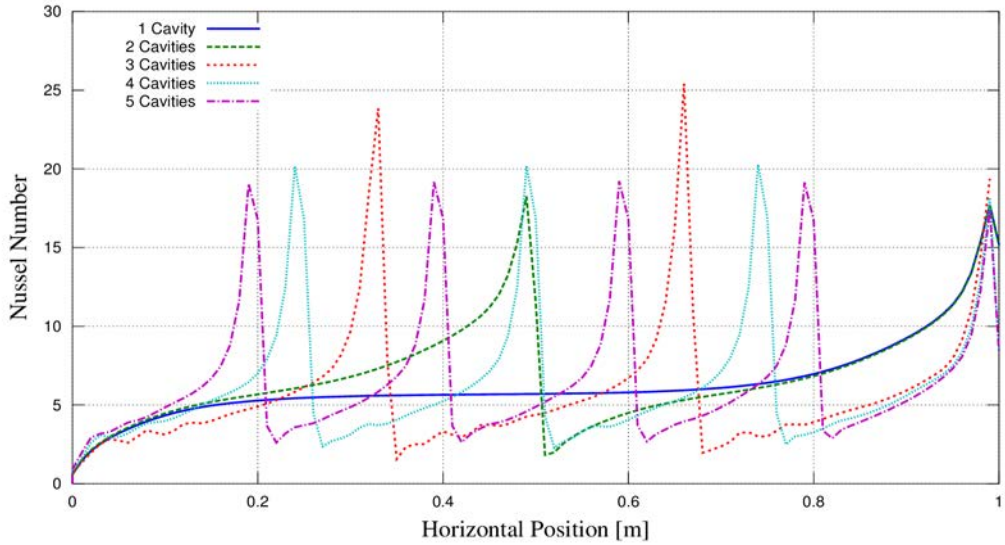

Figure 8: Nusselt number profile on the geometry bottom surface.

ISSN 2176-5480

Table 2: Heat transfer parameter changes for different geometries.

Num. de Cavities	q/A [W/m²]	U_{bt} [W/m² K]	Nu_m
1	174.3	2.39	3.72
2	189.0	2.59	4.03
3	125.0	1.71	2.67
4	132.5	1.82	2.83
5	138.8	1.90	2.96

Results for heat transfer by unit area on these studied geometries and the respective temperatures profile permits the use of wallheatFlux OpenFoam to determine the overall heat flux. Based on this result and the geometry of the problem one can calculate the heat transfer coefficient by the bottom and top surfaces and the average Nusselt number on the bottom surface. These results can be seen in table (2). So, it can be seen that the geometry has three cavities has lowest heat transfer rate. This geometry might be more appropriate to apply as transparent insulation in these cases.

4. CONCLUSIONS

This work shows that there are good alternatives for transparent insulation on solar collectors using baffles in the glass-collector spacing. The study showed that some changes in the flow pattern can contribute significantly on this aspect. Some analyzes were made for a predefined geometry and results from two-dimensional numerical simulation was able to define the existence of an optimal value. In the case of geometry and dimensions analyzed reached the geometry of three cavities as great value. These results should be further verified through experimental procedures, but if validated, may lead to an improvement in the performance of solar collectors without significant increases in costs.

5. ACKNOWLEDGEMENTS

The authors wish thank to CAPES, for financial support to the MSc. student Rafale Paiva Garcia and to UNESP Reitoria for financial support to the undergraduate student Laura Elisa Bollini.

6. REFERENCES

Arulanantham, M. & Kaushika, N., 1996. "Coupled radiative and conductive thermal transfers across transparent honeycomb insulation materials", *Applied Thermal Engineering*, Vol. 16, 209-217.

Avanti, P., Arulanantham, M. & Kaushika, N., 1996. "Solar thermal analysis of transparent-honeycomb-insulated ground collector-storage system", *APPLIED THERMAL ENGINEERING*, Vol. 16, 863-874.

Buchberg, H. & Edwards, D., 1976. "Design considerations for solar collectors with cylindrical glass honeycombs", *Solar Energy*, Vol. 18, 193-203.

Hollands, K., 1965. "Honeycomb Devices in Flat-Plate Solar Collectors", *Solar Energy*, Vol. 9, 159-163.

Hollands, K. & Iynkaran, K., 1993. "Analytical Model for the Thermal Conductance of Compound Honeycomb Transparent Insulation, with Experimental Validation", *Solar Energy*, Vol. 51, 223-227.

Hollands, K. G. T., Unny, T. E., Raithby, G. D. & Konicek, L., 1976. "Free Convective Heat Transfer Across Inclined Air Layers", *Journal of Heat Transfer*, Vol. 98, 189-193.

Incropera, F. P., Witt, D. P., Bergman, T. L. & Lavine, A.S., 2008. *Fundamentos de Transferencia de Calor e Massa*. Editora LTC, 6th edition.

Kaushika, N. & Sharma, P., 1994. "Transparent honeycomb insulated solar thermal systems for energy conservation", *Heat Recovery Systems and CHP*, Vol. 14, 37-44.

Kaushika, N. & Sumathy, K., 2003. "Solar transparent insulation materials: a review", *Renewable and Sustainable Energy Reviews*, Vol. 7, 317-351.

Kaushika, N., Padmapriya, R., Arulanantham, M. & Sharma, P., 1994. "Transparent Insulation Characteristics of Honeycomb and Slat Arrays", *Energy*, Vol. 19, 1037-1041.

ISSN 2176-5480

Malhotra, A., Garg, H. & Rani, U., 1980. "Minimizing convective heat losses in flat plate solar collectors", *Solar Energy*, Vol. 25, 521-526.

OpenFoam Foundation, 2012. . disponible on http://www.openfoam.org/docs/user/.

Platzer, W., 1992. "Calculation Procedure for Collectors with a Honeycomb Cover of Rectangular Cross-Section", *Solar Energy*, Vol. 48, 381-393.

Ruth, D., Hollands, K. & Raithby, G., 1980. "Free-Convection Experiments in Inclined Air Layers Heated from Below", *Journal of Fluid Mechanics*, Vol. 96, 461-472.

Sharma, M. & Kaushika, N., 1987. "Design and Performance-Characteristics of Honeycomb Solar Pond", *Energy Conversion and Management*, Vol. 27, 111-116.

Steinfeld, A. & Schubnell, M., 1993. "Optimum Aperture Size and Operating Temperature of a Solar Cavity-Receiver", *Solar Energy*, Vol. 50, 19-25.

Wong, I. L., Eames, P. C. & Perera, R.S., 2007. "A review of transparent insulation systems and the evaluation of payback period for building applications", *SOLAR ENERGY*, Vol. 81, 1058-1071.

7. RESPONSIBILITY NOTICE

The authors is are the only responsible for the printed material included in this paper.